

The following resources related to this article are available online at www.sciencemag.org (this information is current as of July 20, 2009):

Updated information and services, including high-resolution figures, can be found in the online version of this article at:

<http://www.sciencemag.org/cgi/content/full/324/5928/768>

Supporting Online Material can be found at:

<http://www.sciencemag.org/cgi/content/full/324/5928/768/DC1>

This article **cites 24 articles**, 2 of which can be accessed for free:

<http://www.sciencemag.org/cgi/content/full/324/5928/768#otherarticles>

This article appears in the following **subject collections**:

Chemistry

<http://www.sciencemag.org/cgi/collection/chemistry>

Information about obtaining **reprints** of this article or about obtaining **permission to reproduce this article** in whole or in part can be found at:

<http://www.sciencemag.org/about/permissions.dtl>

width ranged from below 10 nm up to ~150 nm. Chemically derived GNRs were dispersed on a 300-nm SiO₂/Si chip, located and imaged by scanning electron microscopy (SEM) with 1-kV acceleration voltage (13) and by atomic force microscopy (AFM) [Fig. 1, B and C, and fig. S1; see also supporting online material (SOM) (14)].

We then fabricated FET-like devices on selected ribbons with palladium (Pd) metal source/drain (S-D) and highly doped Si backgate (Fig. 1, A and D).

We first focused on GNRs wider than ~20 nm. Under ambient conditions, the edges of these as-made GNRs were probably terminated by

Fig. 1. Electrothermal reaction of individual GNRs in NH₃. **(A)** Schematics of a GNR device e-annealed under high current in NH₃. The devices have metal S-D, highly doped Si backgate and 300-nm SiO₂ gate dielectrics. The color gradient along the GNR represents the temperature profile: higher in the center region and lower near the contacts (18, 25). Atomic colors are as follows: H, green; O, red; N, purple; C, gray. The GNR shown here is assumed to have ideal zigzag edges, which may not correspond to the GNRs in experiments. D, drain; S, source; G, gate. **(B)** SEM (acceleration voltage = 1 kV) and **(C)** AFM images of a ~30-nm-wide GNR. **(D)** AFM image of the device fabricated on the GNR shown in (B) and (C).

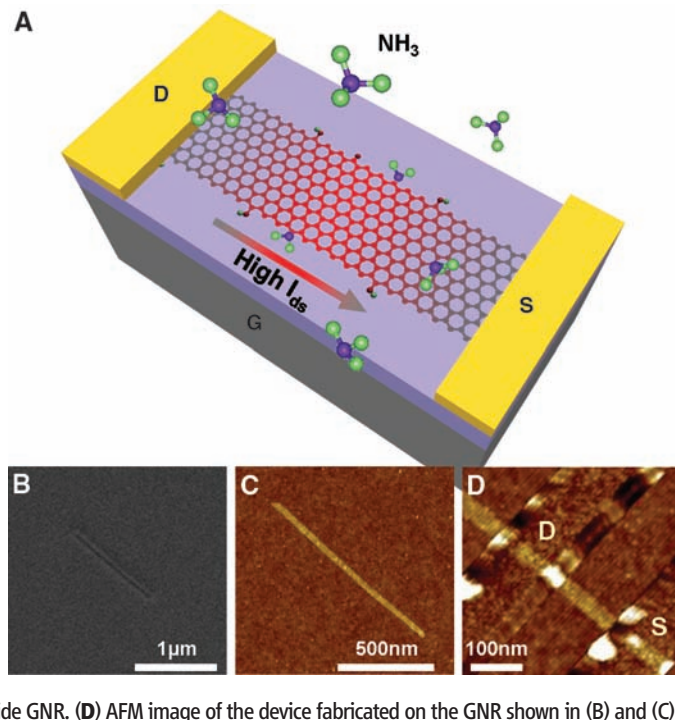
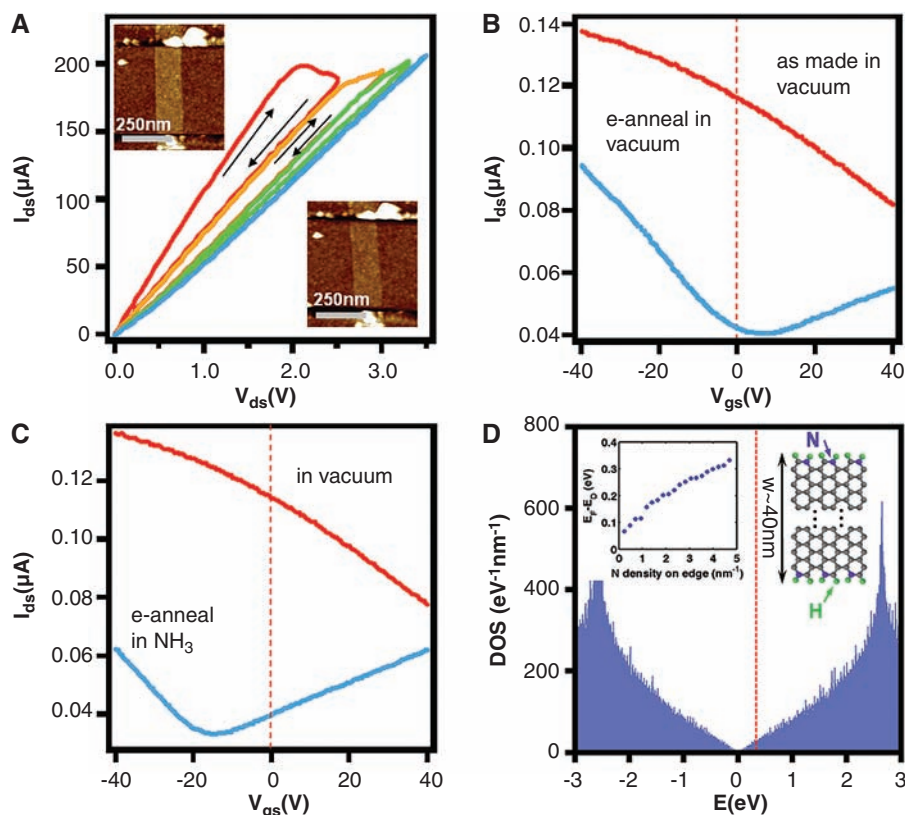


Fig. 2. E-annealing of individual GNRs in vacuum and NH₃. **(A)** Typical e-annealing process in vacuum for a $w \sim 125$ -nm GNR. The process consisted of several double I_{ds} - V_{ds} sweeps (direction pointed by the arrows) with gradually increasing V_{ds} . We stopped when no hysteresis existed between back and forth sweeps (blue curve). (Upper and lower insets) AFM images of the same device as-made and after e-annealing in vacuum, respectively. The height was reduced from ~1.5 to ~1.0 nm because of removal of PmPV coatings by e-annealing. **(B)** I_{ds} - V_{gs} curves of the same GNR device as-made (red) and after e-annealing in vacuum (blue). The Dirac point moved from beyond 40 to ~8 V. **(C)** I_{ds} - V_{gs} curves of the same GNR device in vacuum before (red) and after e-annealing in NH₃ (blue). After e-annealing in NH₃, we pumped the device to base pressure for overnight before taking the blue curve. The Dirac point moved from beyond 40 to ~-14 V. $V_{ds} = 1$ mV in (B) and (C). **(D)** Calculated DOS of a $w \sim 40$ -nm armchair GNR terminated partly by nitrogen species (14). The red dashed line denotes the Fermi level. (Left inset) The dependence of doping level (the position of the Fermi level from the Dirac point) on the density of substitutional N on the edges. (Right inset) Three unit cells of the simulated structure. There are two NH groups in the unit cell of the simulated structure. These edge groups are likely to coexist in real GNRs.



hydrogen, oxygen, hydroxyl groups, and carboxylic groups (15) and exhibited p-doping with the Dirac point at gate voltage $V_{gs} > 40$ V in current-gate voltage I_{ds} - V_{gs} curves [fig. S3 (14)] (1, 2). The p-doping was partly attributed to the oxygen edge groups (6, 7), physisorbed oxygen molecules, and noncovalent poly(m-phenylenevinylene-co-2,5-dioctoxy-p-phenylenevinylene) (PmPV) coatings used in the synthesis process that are known to p-dope carbon nanotubes (16, 17). Pumping in a vacuum reduced the conductance of GNRs slightly [fig. S3 (14)], corresponding to a decrease in p-doping by partial desorption of oxygen, either from the GNRs or GNR-metal contacts (16).

We then e-annealed the devices in high vacuum ($\sim 10^{-6}$ torr) by double sweeping the S-D bias V_{ds} (Fig. 2A). As V_{ds} was increased to high biases, the slope of I_{ds} - V_{ds} curve decreased or even became negative, with a noticeable hysteresis between back-and-forth sweeps that indicated the removal of the p-doping sources (18). We recorded I_{ds} - V_{gs} curves immediately after each e-annealing sweep and observed that the Dirac point gradually moved toward zero V_{gs} [fig. S2 (14)]. We continued to increase V_{ds} during I_{ds} - V_{ds} sweeps until no hysteresis occurred, which indicated that most of the p-doping was removed (Fig. 2A and fig. S2). After e-annealing, the I_{ds} - V_{gs} curve of GNR devices always showed the Dirac point at finite positive V_{gs} (typically 5 to 20 V) and slightly asymmetric hole and electron conduction (Fig. 2B). The residual p-doping was probably caused by oxygen species remaining on the edges (Fig. 3C) (6, 7), as well as the doping

